EUROPEAN ORGANISATION FOR NUCLEAR RESEARCH

CERN-PPE/96-118
August 14, 1996

Search for Neutral Higgs Bosons in Z^0 Decays Using the OPAL Detector at LEP

The OPAL Collaboration

Abstract

A search for neutral Higgs bosons has been performed using the full sample of Z^0 decays collected by the OPAL detector at LEP up to 1995. The data were taken at centre-of-mass energies between 88 GeV and 95 GeV and correspond to an integrated luminosity of approximately 160 pb^{-1}. The present search addresses the processes $Z^0 \to H^0 Z^*$ and $h^0 Z^*$, where H^0 is the Higgs boson predicted by the Standard Model and h^0 the lightest neutral scalar Higgs boson predicted in the framework of the Minimal Supersymmetric Standard Model. For the virtual Z^0 boson, Z^*, the following decay channels are considered: $Z^* \to \nu\bar{\nu}$, e^+e^- and $\mu^+\mu^-$. One candidate event has been found in the $\mu^+\mu^- H^0$ channel. Combined with earlier searches, the present search excludes the SM Higgs boson, at the 95% confidence level (CL), from the mass range below 59.6 GeV. In the framework of the Minimal Supersymmetric Standard Model, allowing a wide range of variation for most relevant model parameters, a 95% CL lower limit of 44.3 GeV is obtained for the mass of the h^0 boson. Combined with earlier direct searches for the Higgs boson pair production process $Z^0 \to h^0 A^0$ and with measurements of the Z^0 line shape, a 95% CL lower limit of 23.5 GeV is obtained for the mass of the pseudoscalar Higgs boson A^0, assuming $\tan\beta \geq 1$.

Submitted to Z. Phys. C.

The OPAL Collaboration

G. Alexander[23], J. Allison[16], N. Altekamp[5], K. Ametewee[25], K.J. Anderson[9], S. Anderson[12], S. Arcelli[2], S. Asai[24], D. Axen[29], G. Azuelos[18,a], A.H. Ball[17], E. Barberio[8], R.J. Barlow[16], R. Bartoldus[3], J.R. Batley[5], J. Bechtluft[14], C. Beeston[16], T. Behnke[8], A.N. Bell[1], K.W. Bell[20], G. Bella[23], S. Bentvelsen[8], P. Berlich[10], S. Bethke[14], O. Biebel[14], V. Blobel[8], I.J. Bloodworth[1], J.E. Bloomer[1], M. Bobinski[10], P. Bock[11], H.M. Bosch[11], M. Boutemeur[34], B.T. Bouwens[12], S. Braibant[12], R.M. Brown[20], H.J. Burckhart[8], C. Burgard[8], R. Bürgin[10], P. Capiluppi[2], R.K. Carnegie[6], A.A. Carter[13], J.R. Carter[5], C.Y. Chang[17], C. Charlesworth[6], D.G. Charlton[1,b], D. Chrisman[4], S.L. Chu[4], P.E.L. Clarke[15], I. Cohen[23], J.E. Conboy[15], O.C. Cooke[16], M. Cuffiani[2], S. Dado[22], C. Dallapiccola[17], G.M. Dallavalle[2], S. De Jong[12], L.A. del Pozo[8], K. Desch[3], M.S. Dixit[7], E. do Couto e Silva[12], M. Doucet[18], E. Duchovni[26], G. Duckeck[34], I.P. Duerdoth[16], J.E.G. Edwards[16], P.G. Estabrooks[6], H.G. Evans[9], M. Evans[13], F. Fabbri[2], P. Fath[11], F. Fiedler[12], M. Fierro[2], H.M. Fischer[3], R. Folman[26], D.G. Fong[17], M. Foucher[17], A. Fürtjes[8], P. Gagnon[7], A. Gaidot[21], J.W. Gary[4], J. Gascon[18], S.M. Gascon-Shotkin[17], N.I. Geddes[20], C. Geich-Gimbel[3], F.X. Gentit[21], T. Geralis[20], G. Giacomelli[2], P. Giacomelli[4], R. Giacomelli[2], V. Gibson[5], W.R. Gibson[13], D.M. Gingrich[30,a], D. Glenzinski[9], J. Goldberg[22], M.J. Goodrick[5], W. Gorn[4], C. Grandi[2], E. Gross[26], M. Gruwé[8], C. Hajdu[32], G.G. Hanson[12], M. Hansroul[8], M. Hapke[13], C.K. Hargrove[7], P.A. Hart[9], C. Hartmann[3], M. Hauschild[8], C.M. Hawkes[5], R. Hawkings[8], R.J. Hemingway[6], G. Herten[10], R.D. Heuer[8], M.D. Hildreth[8], J.C. Hill[5], S.J. Hillier[1], T. Hilse[10], P.R. Hobson[25], R.J. Homer[1], A.K. Honma[28,a], D. Horváth[32,c], R. Howard[29], R.E. Hughes-Jones[16], D.E. Hutchcroft[5], P. Igo-Kemenes[11], D.C. Imrie[25], M.R. Ingram[16], K. Ishii[24], A. Jawahery[17], P.W. Jeffreys[20], H. Jeremie[18], M. Jimack[1], A. Joly[18], C.R. Jones[5], G. Jones[16], M. Jones[6], R.W.L. Jones[8], U. Jost[11], P. Jovanovic[1], T.R. Junk[8], D. Karlen[6], K. Kawagoe[24], T. Kawamoto[24], R.K. Keeler[28], R.G. Kellogg[17], B.W. Kennedy[20], B.J. King[8], J. Kirk[29], S. Kluth[8], T. Kobayashi[24], M. Kobel[10], D.S. Koetke[6], T.P. Kokott[3], M. Kolrep[10], S. Komamiya[24], R. Kowalewski[8], T. Kress[11], P. Krieger[6], J. von Krogh[11], P. Kyberd[13], G.D. Lafferty[16], H. Lafoux[21], R. Lahmann[17], W.P. Lai[19], D. Lanske[14], J. Lauber[15], S.R. Lautenschlager[31], J.G. Layter[4], D. Lazic[22], A.M. Lee[31], E. Lefebvre[18], D. Lellouch[26], J. Letts[2], L. Levinson[26], C. Lewis[15], S.L. Lloyd[13], F.K. Loebinger[16], G.D. Long[17], M.J. Losty[7], J. Ludwig[10], A. Malik[21], M. Mannelli[8], S. Marcellini[2], C. Markus[3], A.J. Martin[13], J.P. Martin[18], G. Martinez[17], T. Mashimo[24], W. Matthews[25], P. Mättig[3], W.J. McDonald[30], J. McKenna[29], E.A. Mckigney[15], T.J. McMahon[1], A.I. McNab[13], R.A. McPherson[8], F. Meijers[8], S. Menke[3], F.S. Merritt[9], H. Mes[7], J. Meyer[27], A. Michelini[2], G. Mikenberg[26], D.J. Miller[15], R. Mir[26], W. Mohr[10], A. Montanari[2], T. Mori[24], M. Morii[24], U. Müller[3], K. Nagai[26], I. Nakamura[24], H.A. Neal[8], B. Nellen[3], B. Nijjhar[16], R. Nisius[8], S.W. O'Neale[1], F.G. Oakham[7], F. Odorici[2], H.O. Ogren[12], T. Omori[24], M.J. Oreglia[9], S. Orito[24], J. Pálinkás[33,d], G. Pásztor[32], J.R. Pater[16], G.N. Patrick[20], J. Patt[10], M.J. Pearce[1], S. Petzold[27], P. Pfeifenschneider[14], J.E. Pilcher[9], J. Pinfold[30], D.E. Plane[8], P. Poffenberger[28], B. Poli[2], A. Posthaus[3], H. Przysiezniak[30], D.L. Rees[1], D. Rigby[1], S.A. Robins[13], N. Rodning[30], J.M. Roney[28], A. Rooke[15], E. Ros[8], A.M. Rossi[2], M. Rosvick[28], P. Routenburg[30], Y. Rozen[22], K. Runge[10], O. Runolfsson[8], U. Ruppel[14], D.R. Rust[12], R. Rylko[25], K. Sachs[10], E.K.G. Sarkisyan[23], M. Sasaki[24], C. Sbarra[2], A.D. Schaile[34], O. Schaile[34], F. Scharf[3], P. Scharff-Hansen[8], P. Schenk[4], B. Schmitt[8],

S. Schmitt[11], M. Schröder[8], H.C. Schultz-Coulon[10], M. Schulz[8], M. Schumacher[3], P. Schütz[3], W.G. Scott[20], T.G. Shears[16], B.C. Shen[4], C.H. Shepherd-Themistocleous[27], P. Sherwood[15], G.P. Siroli[2], A. Sittler[27], A. Skillman[15], A. Skuja[17], A.M. Smith[8], T.J. Smith[28], G.A. Snow[17], R. Sobie[28], S. Söldner-Rembold[10], R.W. Springer[30], M. Sproston[20], A. Stahl[3], M. Starks[12], M. Steiert[11], K. Stephens[16], J. Steuerer[27], B. Stockhausen[3], D. Strom[19], F. Strumia[8], P. Szymanski[20], R. Tafirout[18], S.D. Talbot[1], S. Tanaka[24], P. Taras[18], S. Tarem[22], M. Tecchio[8], M. Thiergen[10], M.A. Thomson[8], E. von Törne[3], S. Towers[6], T. Tsukamoto[24], E. Tsur[23], A.S. Turcot[9], M.F. Turner-Watson[8], P. Utzat[11], R. Van Kooten[12], G. Vasseur[21], M. Verzocchi[10], P. Vikas[18], M. Vincter[28], E.H. Vokurka[16], F. Wäckerle[10], A. Wagner[27], C.P. Ward[5], D.R. Ward[5], J.J. Ward[15], P.M. Watkins[1], A.T. Watson[1], N.K. Watson[7], P. Weber[6], P.S. Wells[8], N. Wermes[3], J.S. White[28], B. Wilkens[10], G.W. Wilson[27], J.A. Wilson[1], G. Wolf[26], S. Wotton[5], T.R. Wyatt[16], S. Yamashita[24], G. Yekutieli[26], V. Zacek[18],

[1]School of Physics and Space Research, University of Birmingham, Birmingham B15 2TT, UK
[2]Dipartimento di Fisica dell' Università di Bologna and INFN, I-40126 Bologna, Italy
[3]Physikalisches Institut, Universität Bonn, D-53115 Bonn, Germany
[4]Department of Physics, University of California, Riverside CA 92521, USA
[5]Cavendish Laboratory, Cambridge CB3 0HE, UK
[6] Ottawa-Carleton Institute for Physics, Department of Physics, Carleton University, Ottawa, Ontario K1S 5B6, Canada
[7]Centre for Research in Particle Physics, Carleton University, Ottawa, Ontario K1S 5B6, Canada
[8]CERN, European Organisation for Particle Physics, CH-1211 Geneva 23, Switzerland
[9]Enrico Fermi Institute and Department of Physics, University of Chicago, Chicago IL 60637, USA
[10]Fakultät für Physik, Albert Ludwigs Universität, D-79104 Freiburg, Germany
[11]Physikalisches Institut, Universität Heidelberg, D-69120 Heidelberg, Germany
[12]Indiana University, Department of Physics, Swain Hall West 117, Bloomington IN 47405, USA
[13]Queen Mary and Westfield College, University of London, London E1 4NS, UK
[14]Technische Hochschule Aachen, III Physikalisches Institut, Sommerfeldstrasse 26-28, D-52056 Aachen, Germany
[15]University College London, London WC1E 6BT, UK
[16]Department of Physics, Schuster Laboratory, The University, Manchester M13 9PL, UK
[17]Department of Physics, University of Maryland, College Park, MD 20742, USA
[18]Laboratoire de Physique Nucléaire, Université de Montréal, Montréal, Quebec H3C 3J7, Canada
[19]University of Oregon, Department of Physics, Eugene OR 97403, USA
[20]Rutherford Appleton Laboratory, Chilton, Didcot, Oxfordshire OX11 0QX, UK
[21]CEA, DAPNIA/SPP, CE-Saclay, F-91191 Gif-sur-Yvette, France
[22]Department of Physics, Technion-Israel Institute of Technology, Haifa 32000, Israel
[23]Department of Physics and Astronomy, Tel Aviv University, Tel Aviv 69978, Israel
[24]International Centre for Elementary Particle Physics and Department of Physics, University

of Tokyo, Tokyo 113, and Kobe University, Kobe 657, Japan
[25]Brunel University, Uxbridge, Middlesex UB8 3PH, UK
[26]Particle Physics Department, Weizmann Institute of Science, Rehovot 76100, Israel
[27]Universität Hamburg/DESY, II Institut für Experimental Physik, Notkestrasse 85, D-22607 Hamburg, Germany
[28]University of Victoria, Department of Physics, P O Box 3055, Victoria BC V8W 3P6, Canada
[29]University of British Columbia, Department of Physics, Vancouver BC V6T 1Z1, Canada
[30]University of Alberta, Department of Physics, Edmonton AB T6G 2J1, Canada
[31]Duke University, Dept of Physics, Durham, NC 27708-0305, USA
[32]Research Institute for Particle and Nuclear Physics, H-1525 Budapest, P O Box 49, Hungary
[33]Institute of Nuclear Research, H-4001 Debrecen, P O Box 51, Hungary
[34]Ludwigs-Maximilians-Universität München, Sektion Physik, Am Coulombwall 1, D-85748 Garching, Germany

[a] and at TRIUMF, Vancouver, Canada V6T 2A3
[b] and Royal Society University Research Fellow
[c] and Institute of Nuclear Research, Debrecen, Hungary
[d] and Department of Experimental Physics, Lajos Kossuth University, Debrecen, Hungary
and OTKA F-015089.

1 Introduction

Local gauge-invariant theories of the electroweak interaction introduce spontaneous symmetry breaking [1] to allow some of the gauge bosons to acquire mass while keeping the theory renormalizable. This procedure predicts the existence of one or more scalar particles, the Higgs bosons [2]. Despite a worldwide experimental effort, these Higgs particles have not yet been discovered.

The simplest such theory, the Standard Model (SM), has one doublet of complex Higgs fields. It predicts the existence of a single scalar Higgs boson (H^0) with unspecified mass but well defined couplings. Consequently, the cross-section for the production of an H^0 in e^+e^- collisions (through the Bjorken process $e^+e^- \to Z^0 \to H^0Z^*$ [3]) and the H^0 decay branching ratios are precisely predicted as a function of the Higgs boson mass, m_{H^0}.

Despite the success of the SM in describing elementary particle phenomena at the electroweak energy scale and below, the theory has considerable shortcomings. For example, it does not predict the mass spectrum and family structure of fermions. There is also the problem of quadratically divergent radiative corrections to the Higgs boson mass often referred to as the "naturalness problem". While in the SM these divergences are cancelled by fine-tuning of model parameters, supersymmetric (SUSY) models [4] provide a more elegant solution: the divergent loops from standard particles are cancelled by equivalent loops of their SUSY partners.

The implementation of SUSY necessitates at least a second doublet of complex Higgs fields. In the Minimal Supersymmetric extension of the Standard Model (MSSM) considered here [5], there are two such doublets, one of which, with vacuum expectation value v_2, couples only to up-type fermions while the other, with vacuum expectation value v_1, couples only to down-type fermions. The ratio $\tan\beta = v_2/v_1$ is a free parameter of the model. While it is expected to be in the range $1 \leq \tan\beta \leq m_t/m_b \approx 40$ (m_t and m_b are the top and bottom quark masses), values slightly less than 1 cannot be excluded a priori [6].

The MSSM predicts an enlarged Higgs sector [5] with five physical Higgs bosons: one pair of charged particles, $H^\pm$, two CP-even neutral scalars, h^0 and H^0 ($m_{h^0} < m_{H^0}$ by definition), and one CP-odd neutral particle, A^0. At the tree level, the masses obey the following relations: $m_{h^0} < m_{Z^0} < m_{H^0}$, $m_{h^0} < m_{A^0} < m_{H^0}$, and $m_{H^\pm} > m_{W^\pm}$. Of these relations the first has perhaps the greatest phenomenological impact since it limits from above the mass of the lightest CP-even Higgs boson, h^0. These mass relations are modified when radiative loop-corrections due to heavy quarks and squarks, in particular the top and stop quarks, are taken into account: m_{h^0} may become larger than m_{Z^0}, and m_{A^0} may become smaller than m_{h^0}. It is important to note, however, that even with two-loop radiative corrections included, the mass of the h^0 boson is constrained to less than approximately 140 GeV. For a recent discussion of the Higgs boson phenomenology at LEP energies, see e.g. Ref. [7] and references quoted therein.

At LEP energies in the vicinity of the Z^0 resonance, the h^0 and A^0 bosons could be produced by the Bjorken process $Z^0 \to h^0Z^*$ and by the Higgs-pair process $Z^0 \to h^0A^0$. In the MSSM the

cross-sections of these processes, σ_{hZ} and σ_{hA}, are related [7] to the cross-section, σ_{HZ}^{SM}, of the SM process $Z^0 \rightarrow H^0 Z^*$ by the relations

$$\sigma_{hZ} = \sin^2(\beta - \alpha)\ \sigma_{HZ}^{SM} \tag{1}$$

$$\sigma_{hA} = \cos^2(\beta - \alpha)\ \bar{\lambda}\ \sigma_{HZ}^{SM} \tag{2}$$

where $\bar{\lambda}$ is a kinematic factor, smaller than 1, which depends on $m_{\mathrm{h^0}}$ and $m_{\mathrm{A^0}}$ and accounts for the suppression of the p-wave cross-section near the production threshold. The coefficients $\sin^2(\beta - \alpha)$ and $\cos^2(\beta - \alpha)$ are determined by the MSSM as a function of the Higgs boson masses and other model parameters (α is a mixing angle relevant for the physical masses of the CP-even Higgs bosons h^0 and H^0).

The results of the four LEP experiments from earlier searches, for the SM Higgs boson [8] [9] [10] and for Higgs bosons in the MSSM [11] [12], together with more recent results, are summarized in Refs. [13] and [14]. Recently ALEPH have updated their limit for the mass of the SM Higgs boson using all data collected at the Z^0 resonance [15]. The latest OPAL publications on searches for the SM Higgs boson [10] and for h^0 and A^0 in the MSSM [12] are based on data collected until the end of 1993, which amount to an integrated luminosity of approximately 75 pb^{-1}. The present update is based on the analysis of more than 5 million Z^0 decays collected by OPAL before the end of 1995, corresponding to an integrated luminosity of approximately 160 pb^{-1}.

In the case of the SM Higgs boson, the search is performed in the missing energy channel ($Z^* \rightarrow \nu\bar{\nu}$ and $H^0 \rightarrow q\bar{q}$) and in the charged lepton channel ($Z^* \rightarrow e^+e^-$ or $\mu^+\mu^-$ and $H^0 \rightarrow q\bar{q}$). Other channels previously exploited, namely ($Z^* \rightarrow \tau^+\tau^-$)($H^0 \rightarrow q\bar{q}$), ($Z^* \rightarrow q\bar{q}$)($H^0 \rightarrow \tau^+\tau^-$) and ($Z^* \rightarrow \nu\bar{\nu}$)($H^0 \rightarrow \tau^+\tau^-$) have been discarded for reasons of high background. In the missing energy and charged lepton channels the event selection has been improved since Refs. [10] and [12] to yield better rejection against backgrounds which have become important at the present high integrated luminosities. The new search in the missing energy channel is described in a recent publication [16]. We quote the results since these are relevant to the present update. The new search in the charged lepton channel is discussed in this paper. There, a detailed study of the backgrounds was necessary to establish whether this channel still has the required sensitivity to contribute to the search at Higgs boson masses in the vicinity of 60 GeV.

The interpretation of the earlier searches for the MSSM Higgs bosons h^0 and A^0 is also updated. The results obtained for the SM Higgs boson are interpreted as searches for the process $Z^0 \rightarrow h^0 Z^*$ using Equation (1). For the process $Z^0 \rightarrow h^0 A^0$ the update relies on searches published earlier [12]. Although these are based on the smaller data sample that was available at the end of 1993, their range of sensitivity extended very close to the kinematic limit of the process, $m_{\mathrm{h^0}} + m_{\mathrm{A^0}} = m_{\mathrm{Z^0}}$. While the earlier results, based on the effective potential approximation [17], were strictly valid only in a rather restricted theoretical framework of the MSSM (e.g. the masses of all SUSY particles were assumed to be degenerate and described by a single mass parameter), the present results are derived using solutions of the renormalization group equations [18] and allow for variations of the relevant MSSM parameters over wide ranges expected from theory. The new results also make use of a better knowledge of the top quark mass [19] and of restrictions of the parameter space which are derived from experimental limits on

SUSY particle masses. Note that the search in the missing energy channel described in Ref. [16] is also sensitive to final states where the h^0 boson decays into "invisible" channels such as $h^0 \to \tilde{\chi_1}^0 \tilde{\chi_1}^0$ which may have a sizeable branching fraction in the MSSM ($\tilde{\chi_1}^0$ is the lightest neutralino, assumed to be the lightest supersymmetric particle). Such final states were not considered to exist in the previous publication.

The OPAL detector is described in detail in Ref. [20]. It is a multipurpose apparatus having nearly complete solid angle coverage. The central detector consists of a system of tracking chambers providing charged-particle tracking over 96% of the full solid angle inside a 0.435 T solenoidal magnetic field. Besides measuring particle momenta, the central detector also contributes to the identification of particles by measuring the specific ionization loss, $\mathrm{d}E/\mathrm{d}x$, in the chamber gas. A silicon microstrip detector with two layers [21], surrounding the beam-pipe, provides precision measurements of track impact parameters and the reconstruction of secondary decay vertices. A lead-glass electromagnetic calorimeter located outside the magnet coil covers the full azimuthal angle range with excellent hermeticity in the polar angle range $|\cos\theta| < 0.82$ for the barrel region and $0.81 < |\cos\theta| < 0.984$ for the endcap region (the polar angle θ is defined with respect to the e^- beam direction). The magnet return yoke is instrumented for hadron calorimetry, and consists of barrel and endcap sections along with pole tips that together cover the region $|\cos\theta| < 0.99$. Calorimeters close to the beam axis measure the luminosity using small angle Bhabha scattering events and complete the geometrical acceptance down to 26 mrad. These include the forward detectors (FD) which are lead-scintillator sandwich calorimeters, and at smaller angles, since 1993, silicon-tungsten calorimeters (SW) [22] located on both sides of the interaction point.

The signal detection efficiencies and possible backgrounds to the missing energy and charged lepton channels are studied by extensive Monte Carlo simulations. The generated event samples are passed through a detailed simulation of the OPAL detector [23] and processed in the same manner as the data.

The next two sections summarize the searches in the missing energy and the charged lepton channels. The results are combined in Section 4 where an updated mass limit is presented for the SM Higgs boson. In Section 5 the results are interpreted in the MSSM and updated mass limits for the h^0 and A^0 bosons are presented.

2 Search for Higgs bosons in missing energy channels

The data are searched for events with sizeable missing energy and a visible part which consists either of a hadronic "monojet" or a hadronic acoplanar "dijet" (i.e. two jets which are not back-to-back in the plane transverse to the colliding beams). Such event topologies would arise not only in the SM process $Z^0 \to H^0 Z^*$ but also in $Z^0 \to h^0 Z^*$ followed by $Z^* \to \nu\bar{\nu}$, and in the process $Z^0 \to h^0 Z^*$ followed by $(h^0 \to \tilde{\chi_1}^0 \tilde{\chi_1}^0)(Z^* \to \text{hadrons})$. The monojet topology occurs when the invisible part of the event ($Z^0 \to \nu\bar{\nu}$ or $h^0 \to \tilde{\chi_1}^0 \tilde{\chi_1}^0$) has a large invariant mass while the dijet topology characterizes events with low invisible mass, typically less than 25 GeV.

The selection criteria for these event topologies are described in Ref. [16]. In order to classify an event as monojet or dijet, it is divided into two hemispheres by the plane orthogonal to the thrust axis. If there are no tracks and clusters passing basic quality requirements in one of the hemispheres, the event is classified as monojet; otherwise it is classified as dijet. Dijet events are then required to exhibit significant acoplanarity. The event selection leaves two events in the data sample while the simulation of the various backgrounds, mainly from $Z^0 \rightarrow$ hadrons, $\tau^+\tau^-$, and from higher-order four-fermion processes, predicts 2.3 ± 0.4 events. The two observed events are therefore compatible with background expectations. However, they are considered as signal candidates when mass limits are derived. The first candidate, a dijet, has a visible mass of 24.8 ± 3.0 GeV and an invisible mass of 34.9 ± 7.7 GeV. The second candidate, a monojet, has a visible mass of 6.3 ± 0.8 GeV and an invisible mass of 78.5 ± 1.3 GeV.

In the case of visible Higgs boson decays (and invisible Z^* decays) the detection efficiencies vary from 30% for a Higgs boson mass of 12 GeV to 50% at 40 GeV, decreasing to 15% at 65 GeV. For the case of an invisible Higgs boson (and a visible $Z^* \rightarrow q\bar{q}$ decay) it is 26% for Higgs bosons with mass less than 5 GeV, rising to 55% at 50 GeV and falling to 22% at 70 GeV. The combined statistical and systematic errors which affect these efficiencies range from 2% at low to 6% at high visible mass.

3 Search for Higgs bosons in the charged lepton channel

The experimental signature for the process $e^+e^- \rightarrow Z^0 \rightarrow H^0 Z^*$ followed by $Z^* \rightarrow (e^+e^-$ or $\mu^+\mu^-)$ and $H^0 \rightarrow q\bar{q}$ is a pair of well isolated, energetic, oppositely charged leptons produced together with a high-mass hadronic system. The data selection follows closely that described in an earlier publication [10]. However, the old selection criteria have been tightened and new requirements were added to cope with the increased luminosity of the data, which requires a better rejection of backgrounds while keeping a high detection efficiency for the signal, especially for large Higgs boson masses. It was therefore important to achieve a better understanding of the backgrounds, mainly from hadronic Z^0 decays and from higher-order four-fermion processes. The latter, although low in rate, may have event topologies very similar to those of the signal.

The signal is simulated using the PYTHIA event generator [24]. To study the backgrounds, the following event samples are used: (i) about 4 million hadronic Z^0 decays generated by JETSET [24] with the relevant parameters which govern the hadronization process tuned to OPAL data [25]; (ii) 160 000 four-fermion events (80 000 for each of the final states $e^+e^-q\bar{q}$ and $\mu^+\mu^-q\bar{q}$) generated by FERMISV [26] which adequately describes the measured OPAL data [27]; (iii) a large sample of JETSET $Z^0 \rightarrow b\bar{b} \rightarrow e^+e^-X$, $\mu^+\mu^-X$ (inclusive e^+e^- and $\mu^+\mu^-$ events) having more than 10 times the statistics of the data.

It is difficult to predict accurately the background from hadronic Z^0 decays, because the events which mimic the signal topology form an extremely small fraction of such decays. Our strategy is to apply stringent cuts against such events, with a high degree of redundancy, so as to reduce the background to a negligible level. The following modifications are applied to the

analysis of Ref. [10]:

- The requirements to identify electrons and muons are tightened. This reduces the probability for misidentifying hadrons as leptons. For the e^+e^- channel, the requirement on the specific ionization loss, dE/dx, of a charged particle in the central detector gas is changed from $dE/dx > 9.17$ keV/cm to $9.17 < dE/dx < 12.0$ keV/cm, and the requirement on the ratio of particle energy over momentum changed from $E/p > 0.7$ to $0.7 < E/p < 3.0$. For the $\mu^+\mu^-$ channel, tight requirements were applied in the previous analysis to only one of the muons and looser requirements to the second muon [10] whereas now the same tight requirements are applied to both muons.

- The energy measured in the forward and silicon-tungsten calorimeters is used to veto two-photon events and hadronic Z^0 decays with one of the jets emitted at small polar angle. Previously only the FD calorimeters were used. In the present analysis the FD and SW calorimeter are used in conjunction for the data taken since the SW detector was installed.

Other modifications improve the quality of the selection and compensate for the losses in signal detection efficiency which are caused by the tighter requirements described above.

- The cut on the hadronic mass, at 25 GeV, applied formerly to the invariant mass of the hadronic system, with a mass resolution of about 10 GeV, is replaced by a cut using the recoil mass (i.e. the mass of the hadronic system computed as the mass recoiling against the lepton pair), which has a mass resolution of 1 GeV.

- The cut on the scalar-momentum sum of the two muons or the energy sum of the two electrons is lowered from 25 GeV to 20 GeV. This increases the detection efficiency for Higgs bosons with high mass.

As a net result of the above changes, the background from hadronic Z^0 decays has been reduced, while that from four-fermion events has increased. Four new cuts are introduced. The first two are in part redundant with the earlier selection [10] and aim to reduce further the background from hadronic Z^0 decays. In particular, they ensure that all simulated hadronic Z^0 decays are removed by at least two different cuts.

- In the Higgs boson process, the leptons emerge from the primary interaction vertex since they originate from the decay of the Z^* boson. In hadronic Z^0 decays, the leptons tend to originate from a secondary vertex since they mostly come from the decay of a b- or c-flavoured hadron. A cut, $\sqrt{d_1^2 + d_2^2} < 50$ μm, is applied to the sum of the impact parameters in the transverse plane of the two lepton tracks with respect to the primary vertex, added in quadrature. The corresponding distributions for simulated signal and background samples are shown in Figure 1(a).

- Leptons from hadronic Z^0 decays are commonly accompanied by energetic neutrinos which reduce the visible energy of the events. The visible energy obtained from combining track momenta and energies measured in the electromagnetic and hadron calorimeters (a description of the energy-flow algorithm can be found e.g. in Ref. [28]) is required to be larger than 80 GeV; see Figure 1(b).

Finally, two cuts enhance the Higgs boson signal with respect to the remaining four-fermion background:

- Since Higgs bosons decay mainly into $b\bar{b}$ hadronic final states, at least one secondary vertex is required in the event, formed by three or more tracks [29] and having $\delta \equiv \ell/\sigma_l > 3$ (ℓ is the decay length, i.e. the distance between the primary and the secondary vertex in the transverse plane, and σ_l the error on ℓ). See Figure 1 (c) for the corresponding distributions.
- In addition to the previous requirement that both lepton momenta exceed 5 GeV, it is also required that they be less than 30 GeV; see Figure 1 (d).

The effects of the above cuts on the data, on the main sources of background and on the signal from a Higgs boson with 60 GeV mass, are listed in Table 1.

Figure 2 shows distributions of the decay length, δ, and the dilepton mass after all cuts except the one that is applied to the quantity displayed. The cuts on these two quantities have the largest impact on the four-fermion background. Figure 3 shows the recoil mass distributions in the e^+e^- and $\mu^+\mu^-$ channels for the four-fermion background when all selection cuts are applied. In the e^+e^- channel no event survives the selection while in the $\mu^+\mu^-$ channel one candidate event remains; it is indicated by the solid dot. This event, already described in Ref. [10], has a recoil mass of 61.2 ± 1.0 GeV. Further, it has $\sqrt{d_1^2 + d_2^2} = 3.2$ μm, a visible energy of 95 GeV, $\delta = 3.6$ and muon momenta of 19.3 GeV and 7.3 GeV (small deviations from the values quoted in Ref. [10] are mainly due to the improved calibration of the detector).

After all selection cuts, the background from hadronic Z^0 decays is negligible. From applying the selection cuts to the high-statistics sample of simulated $Z^0 \to b\bar{b}$ events one estimates a rejection better than 2.5×10^{-8} against hadronic Z^0 decays having two genuine electrons or muons. The background from fake leptons [1] has been determined as follows. From the sample of 4 million generated hadronic Z^0 decays, a subsample has been selected where the lepton identification requirements were not applied and where the lepton isolation criteria (see: Ref. [10]) were loosened. By applying the lepton identification requirements to that sample one obtains a rejection factor of 7×10^{-4}. On the other hand, by applying all cuts but the lepton identification requirements to the full sample, one obtains a rejection factor of 2×10^{-6}. Thus, the total rejection factor for hadronic Z^0 decays with fake leptons is of the order of 10^{-9}.

[1] Electrons may be faked by a charged hadron overlapping with a photon or a π^0, or by photons converting in the detector material. Muons may be faked by the "punch-through" of charged pions or kaons which give a signal in the muon detectors, or by pions or kaons decaying in flight.

Table 1: Effects of the cuts of the e^+e^- and $\mu^+\mu^-$ selections on the data, the simulated background samples from hadronic Z^0 decays and four-fermion processes, and on the detection efficiency for a Higgs boson with 60 GeV mass. The numbers of events in the simulated background samples are normalized to the integrated luminosity of the data. In the case of the data, requirements on the status of those subdetectors which are relevant for the e^+e^- and $\mu^+\mu^-$ selections introduce a small difference in the number of preselected events.

	e^+e^- selection				$\mu^+\mu^-$ selection			
	Events			$\epsilon(\%)$	Events			$\epsilon(\%)$
	Data	$Z^0 \rightarrow$ had	four-f	Higgs	Data	$Z^0 \rightarrow$ had	four-f	Higgs
Preselection	314 538	292 740	45.4	76.1	316 083	292 740	29.7	81.2
Common cuts	156 146	162 208	31.9	59.7	153 100	162 208	21.6	67.1
Lepton identification	706	622	10.2	49.6	2 139	1 790	8.7	60.5
Lepton isolation	11	0	8.8	38.0	9	1.0	7.2	45.6
$\ell^+\ell^-$ and recoil mass	7	0	3.8	34.7	4	1.0	2.9	42.8
$\sqrt{d_1^2 + d_2^2}$	6	0	3.6	33.8	4	1.0	2.8	41.9
Visible energy	4	0	3.0	28.5	3	0.0	2.7	39.0
ℓ/σ_ℓ	1	0	0.6	21.5	1	0.0	0.5	30.8
Lepton momentum	0	0	0.4	21.5	1	0.0	0.4	30.8

Table 2: Efficiencies for the e^+e^- and $\mu^+\mu^-$ selections, number of Higgs bosons expected to be produced ($N_{prod}^{e^+e^-,\mu^+\mu^-}$) and to be detected experimentally ($N_{exp}^{e^+e^-,\mu^+\mu^-,total}$), as a function of the Higgs boson mass.

m_{H^0} [GeV]	$\epsilon_{e^+e^-}(\%)$	$\epsilon_{\mu^+\mu^-}(\%)$	$N_{prod}^{e^+e^-}$	$N_{prod}^{\mu^+\mu^-}$	$N_{exp}^{e^+e^-}$	$N_{exp}^{\mu^+\mu^-}$	N_{exp}^{total}
30	9.8	8.6	71.4	71.6	6.9	6.2	13.1
40	22.1	23.1	26.5	26.6	5.9	6.1	12.0
50	24.2	33.6	8.3	8.4	2.0	2.8	4.8
54	25.3	29.4	5.1	5.1	1.3	1.5	2.8
56	24.5	29.9	3.7	3.8	0.9	1.1	2.0
58	23.2	28.0	2.8	2.8	0.6	0.8	1.4
60	21.5	30.8	2.0	2.0	0.4	0.6	1.0
62	20.8	23.8	1.4	1.4	0.3	0.3	0.6
66	17.1	21.6	0.6	0.6	0.1	0.1	0.2

If one considers only events with recoil mass larger than 50 GeV, i.e. with masses in the vicinity of, or higher than, the Higgs boson mass limit quoted in Ref. [10], the residual background after all selection cuts is 0.17 ± 0.02 events in the e^+e^- channel and 0.21 ± 0.03 events in the $\mu^+\mu^-$ channel.

The signal detection efficiencies are listed in Table 2 as a function of the Higgs boson mass. The last column shows the expected number of signal events in the e^+e^- and $\mu^+\mu^-$ channels combined. These numbers have an error of about 7%, from Monte Carlo statistics (5%), from uncertainties on the integrated luminosity (1%) and the production cross-section (1%) and from uncertainties which affect the simulation of the selection requirements (5%).

4 Mass limit for the SM Higgs boson

The numbers of expected signal events in the missing energy channel and in the charged lepton channel (e^+e^- and $\mu^+\mu^-$ combined), and their sum, are listed in Table 3 as a function of the Higgs boson mass. To derive a mass limit, the expected numbers of events are to be compared to the 95% CL upper limit which is derived from the observation in the data; see Figure 4. Before the comparison, the expected numbers of events are decreased by their systematic errors.

Taking the missing energy channel by itself, the two observed events are far below the mass limit of Ref. [10]. Their influence on the new mass limit is negligible. For zero observed events in the proximity of the mass limit one obtains in this case a 95% CL lower limit of 60.6 GeV for the mass of the SM Higgs boson [16]. Taking the leptonic channel separately, the observed

Table 3: Efficiencies (%) and expected numbers of events for the missing energy ($\nu\bar{\nu}$) and charged lepton channels, and their sums.

$m_{\mathrm{h^0}}$ [GeV]	$\epsilon^{\nu\bar{\nu}}(\%)$	$N_{exp}^{\nu\bar{\nu}}$	$\epsilon^{\ell^+\ell^-}(\%)$	$N_{exp}^{\ell^+\ell^-}$	N_{exp}^{total}
30	47.7	203.8	9.2	13.1	216.9
40	51.6	84.0	22.6	12.0	96.0
50	38.6	20.4	28.9	4.8	25.2
54	33.1	10.8	27.3	2.8	13.6
55	31.7	8.7	27.3	2.0	10.7
56	30.5	7.4	27.2	1.8	9.2
58	28.7	5.2	25.6	1.4	6.6
60	25.7	3.4	26.1	1.1	4.5
62	21.4	2.1	22.3	0.6	2.7
65	15.1	0.8	19.6	0.3	1.1
66	13.0	0.6	19.4	0.2	0.8

$\mu^+\mu^-\mathrm{H^0}$ candidate at 61.2$\pm$1.0 GeV mass is well above the limit that can be derived from this channel alone; see Figure 4. The same procedure as in the missing energy channel thus leads to a 95% CL lower limit of 53.2 GeV.

If the missing energy and leptonic channels are combined, one has to take into account the observed candidate in the $\mu^+\mu^-\mathrm{H^0}$ channel since the mass of that event is sufficiently close to the limit to have an impact on its value. One obtains in this case 59.6 GeV. The joint limit is thus weaker than the one obtained from the missing energy channel alone. Methods with various degrees of sophistication are found in the literature to determine the limit in the presence of candidate events, which take into account the resolution with which the mass of the candidate events is measured (see e.g. Ref. [15], [16]). In the present case these methods give results within only a few hundred MeV of the quoted value. Since uncertainties e.g. from initial-state radiation or from the absolute energy calibration of the detector are of the same order of magnitude, we choose not to apply those methods.

It is pertinent to ask if the leptonic channel still has the required sensitivity to serve as a search channel for Higgs bosons in the mass range close to 60 GeV. To answer this question one uses the Monte Carlo predictions for the signal and background, and compares the luminosity that is required (using the prescription of Ref. [7]) with and without the charged lepton channel, to exclude a signal at the 95% CL. The comparison is done at a Higgs boson mass of 60.6 GeV, i.e. at the mass limit derived from the missing energy channel alone. The predicted signal is 3.0 events in the missing energy channel and 0.9 events in the charged lepton channel. For the background one integrates the predicted number over the range with mass larger than 50 GeV, and obtains 0.6 events in the missing energy channel [16] and 0.4 events in the charged

lepton channel. Using these numbers, the comparison favours the inclusion of the charged lepton channel, although detailed predictions depend crucially on the background estimation. We therefore consider the charged lepton channel with its superior mass resolution to be a sensitive search channel at Higgs boson masses in the vicinity of 60 GeV, and quote the value from the combined analysis, 59.6 GeV, as our best estimate for the lower limit of the SM Higgs boson mass, at the 95% CL.

5 Experimental limits in the MSSM parameter space

In this section we summarize the restrictions on the MSSM parameter space which can be obtained from the searches for the processes $Z^0 \to h^0 Z^*$ and $Z^0 \to h^0 A^0$ and from other experimental inputs.

The cross-sections for the two processes are related to the SM Higgs boson production cross-section by Equations (1) and (2). The SUSY factors $\sin^2(\beta-\alpha)$ and $\cos^2(\beta-\alpha)$ which depend on the MSSM parameters are computed, together with all Higgs boson masses and couplings, from the renormalization group equations at the two-loop level, which have been incorporated into the Higgs boson generator HZHA [30] following Ref. [31]. The following MSSM parameters serve as input to the calculation:

- m_{A^0}, the mass of the pseudoscalar Higgs boson A^0;
- $\tan\beta$;
- M, the universal gaugino mass parameter; $M = M_1 \cos^2\theta_W + M_2 \sin^2\theta_W$, where M_1 and M_2 are the U(1) and SU(2) gaugino masses, respectively, at the electroweak energy scale and θ_W is the weak mixing angle. We remind the reader that M, together with μ and $\tan\beta$ determine the chargino and neutralino mass spectrum;
- μ, the parameter describing the mixing of the two Higgs field doublets;
- A_t, A_b and A_τ, mixing parameters relevant for the stop, sbottom and stau masses at the electroweak energy scale;
- M_q, M_u, M_d, M_l, M_e, soft symmetry breaking mass parameters relevant for the squark and slepton spectra at the electroweak energy scale.

In a complete study of the MSSM parameter space one would have to vary all parameters independently and compare in each case the model prediction to the data. This is difficult since the number of parameter sets to study would be very large. The number of sets is reduced by requiring $A_t = A_b = A_\tau = A$, which implies the same mixing in the stop, the sbottom and the stau sectors. The effect of this simplification on the Higgs mass spectrum is small. It is also assumed that M_q, M_u, M_d, M_l and M_e are all equal to a single parameter, M_S, which implies mass degeneracy of all squarks and sleptons at the electroweak energy scale. Since M_S

is scanned over a wide range, this simplification should not limit the validity of the results. Furthermore, since neither sleptons nor squarks have been detected in Z^0 decays, the impact of these assumptions on Higgs boson decay properties is not important for the currently examined Higgs mass ranges.

In the present study one assumes further that A, M_S and μ are linked by one of the following three sets of relations which correspond to small, intermediate and large deviations from mass degeneracy in the heavy squark sector. The assumed relations are:

- $A = 0,\ \mu = -50$ GeV for small mixing;
- $A = M_S,\ \mu = -M_S$ for intermediate mixing;
- $A = M_S\sqrt{6},\ \mu = -50$ GeV for large mixing.

The heavy squark sector may have considerable impact on the Higgs sector via loop corrections, and it is assumed that the three choices [7] taken together comprise a sufficiently large range of theoretical possibilities. In Ref. [7] the value $\mu = 0$ is proposed for the cases of small and large mixing. However, that value is already excluded to a large extent at LEP [32] since it generates in general small chargino masses. This motivates our choice of $\mu = -50$ GeV, which is the negative value closest to zero that typically yields chargino masses in excess of 40 GeV within the considered range of M. For small values of M_S, this value of μ does not comply to the usual criteria of "minimal" mixing, as defined in Ref. [7], i.e. $\mid \mu \mid << M_S$. Since in the quoted reference the best exclusions are obtained for minimal mixing, the case designated here as small mixing can be considered conservative in comparison.

With these assumptions, the only independent model parameters are $m_{\mathrm{A^0}}$, $\tan\beta$, M and M_S for which large ranges are investigated. The top quark mass is added as a supplementary parameter since the Higgs boson masses depend strongly ($\approx m_t^4$) on the latter. Based on the current experimental findings, m_{t}=175$\pm$9 GeV [19], it is taken [2] as 175, 185 and 195 GeV. The precise parameter values used in the scan are summarized in Table 4. One observes that for each of the three squark mixing scenarios the number of parameter sets considered is approximately 250 000.

For any combination of the input parameters, the HZHA program calculates the Higgs boson (and SUSY particle) masses and couplings, from which detailed decay patterns are derived. For those decays which lead to one of the event topologies listed in Section 5.1 below, the numbers of events expected from the model are compared to the experimental upper limits which are derived, at the 95% CL, from the negative outcome of the searches. The combinations of MSSM parameters are validated or invalidated on the basis of that comparison.

To obtain exclusion contours in the ($m_{\mathrm{h^0}}$,$m_{\mathrm{A^0}}$) projection of the MSSM parameter space, one scans over $m_{\mathrm{h^0}}$ and $m_{\mathrm{A^0}}$ and examines all parameter combinations which yield values

[2] Since the loop-corrections depend strongly on m_{t} we take the central value, and that value increased by 1$\times$ and 2$\times$ the experimental error.

Table 4: List of values of the MSSM parameters and of the top quark mass which are used in the scan.

Small mixing: Intermediate mixing: Large mixing:	$A = 0$, $\mu = -50$ GeV $A = M_S$, $\mu = -M_S$ $A = M_S\ \sqrt{6}$, $\mu = -50$ GeV	
$m_{\mathrm{A^0}}$ [GeV] :	2, 4, 6, ..., 58, 60, 65, 70, 75, 80, 100, 120, 140	37 steps
$\tan\beta$:	0.5, 0.6, 0.7, 0.8, 0.9, 1.10, 1.18, 1.27, 1.37, 1.48, 1.60, 1.73, 1.89, 2.06, 2.27, 2.51, 2.81, 3.18, 3.65, 4.26, 5.12, 6.41, 8.57, 12.8, 25.6	25 steps
M_S [GeV] :	10, 45, 95, 145, 210, 410, 610, 810, 1010	9 steps
M [GeV] :	5, 20, 35, 50, 65, 100, 300, 500, 700, 900	10 steps
m_t [GeV]	175, 185, 195	3 steps

of $m_{\mathrm{h^0}}$ and $m_{\mathrm{A^0}}$ within ± 1 GeV of the chosen masses. The point ($m_{\mathrm{h^0}}$,$m_{\mathrm{A^0}}$) is excluded if none of the parameter combinations is compatible with the experimental upper limits. The precise exclusion limits are obtained by interpolation between the expected numbers of events in adjacent bins.

5.1 Experimental inputs

The experimental restrictions on the MSSM parameter sets are from the following sources:

(a) A first input is the lower limit obtained for the mass of the SM Higgs boson using the missing energy and the charged lepton channels, applied to $m_{\mathrm{h^0}}$ using Equation (1). The missing energy channel, besides being sensitive to visible $\mathrm{h^0}$ decays, is also sensitive to invisible final states, for example the decay $\mathrm{h^0}\rightarrow\tilde{\chi_1}^0\tilde{\chi_1}^0$. As previously mentioned, these searches leave two candidate events in the missing energy channel and one candidate event in the leptonic channel. The corresponding Higgs boson candidate masses are 6.3 ± 0.8 GeV, 24.8 ± 3.0 GeV and 61.2 ± 1.0 GeV. These events are treated as signal events: the 95% CL upper limit is raised locally (within $\pm 2\sigma$ of the observed mass) from 3 events (no candidate) to 4.7 (1 candidate). In the domain where the decay $\mathrm{h^0}\rightarrow\mathrm{A^0A^0}$ is kinematically possible, the selection criteria in the missing energy channel are also applied to the processes $(\mathrm{h^0}\rightarrow\mathrm{A^0A^0})(\mathrm{Z^*}\rightarrow\nu\bar{\nu})$ with the $\mathrm{A^0}$ boson decaying into $\mathrm{q\bar{q}}$ or $\tau^+\tau^-$ final states. However, since the searches in those channels were performed in 1993, they only apply to a reduced data sample. The detection efficiencies are typically lower than for the $\nu\bar{\nu}\mathrm{q\bar{q}}$ final state. For example, at $m_{\mathrm{h^0}}$=50 GeV and $m_{\mathrm{A^0}}$=20 GeV, the $\nu\bar{\nu}\mathrm{q\bar{q}q\bar{q}}$ efficiency is 25% [12].

(b) Another experimental input is provided by various direct searches for the process $Z^0 \to h^0 A^0$. These searches, described in Ref. [12], cover many final states such as purely hadronic events, hadronic events including one or two $\tau^+\tau^-$ pairs, $3(\tau^+\tau^-)$ and $3(b\bar{b})$. Published in 1994, these searches are based on a data sample of 75 pb^{-1} luminosity only. However, their sensitivity extends very close to the kinematic limit, $m_{h^0}+m_{A^0}=m_{Z^0}$. In the quoted publication special attention was devoted to the domain $m_{A^0} < 2m_\tau$ where the A^0 decays are model-dependent and uncertain.

(c) The observed decay width of the Z^0 boson provides another constraint. Compared to the SM prediction, it yields an experimental upper limit of $\Gamma < 13.9$ MeV (95% CL) [33] for any non-standard Z^0 decay channel. Applied to the $Z^0 \to h^0 A^0$ process, it provides at each point of the (m_{h^0},m_{A^0}) plane an upper limit for $\cos^2(\beta-\alpha)$; see Equation (2).

(d) Finally, constraints from experimental limits for supersymmetric particles obtained by OPAL are also used. MSSM parameter combinations which yield SUSY particle masses incompatible with the measured limits are discarded. The strongest restriction is provided by the chargino mass limit which was recently upgraded from 45 GeV (LEP I limit) to $m_{\tilde{\chi}^\pm} > 65$ GeV (see Ref. [32] for the details concerning the restricted applicability of those limits). The direct searches for sleptons and sneutrinos in Z^0 decay [34] restrict M_S to values larger than ≈ 10 GeV. The neutralino mass is restricted to more than 12.5 GeV for $\tan\beta > 1.5$ [16]. The stop mass is required to be heavier than the neutralino which is assumed to be the lightest SUSY particle. Raising the lower limit on the stop mass to 50 GeV [35] has negligible effect on the results.

5.2 Mass limits for the MSSM Higgs bosons h^0 and A^0

The results are presented in Figures 5, 6 and 7 separately for the cases of small, intermediate and large squark mixing. In each case, 95% CL exclusion limits [3] are given in the (m_{h^0},m_{A^0}) plane (parts (a) and (b)), the $(m_{h^0},\tan\beta)$ plane (part (c)) and in the $(m_{A^0},\tan\beta)$ plane (part (d)). Results are given for $\tan\beta \geq 1$ and various values of the top quark mass (parts (a)) and for m_t fixed at 175 GeV and various lower bounds for $\tan\beta$ (part (b)). The lower limits obtained for m_{h^0} and m_{A^0} are listed in Table 5. For m_{h^0} the limit is basically determined by the kinematic limit of the process $Z^0 \to h^0 A^0$and is almost independent of model assumptions. For m_{A^0}, the most conservative (i.e. lowest) limits are obtained in the case of large mixing and large top quark mass.

A word of caution is to be added. It has been pointed out [36] that in the (m_{h^0},m_{A^0}) region beyond the kinematic limit of the process $Z^0 \to h^0 A^0$, for $m_{h^0}+m_{A^0} > m_{Z^0}$, the cross-section for $Z^0 \to h^0 Z^*$ may become very small for some particular sets of the MSSM parameters. Such sets cannot be excluded at present centre-of-mass energies. The parameter combinations considered in this analysis, specified in Table 4, do not reveal any such cases.

[3] In the figures the experimental exclusion contours are combined with the theoretical bounds of the MSSM which correspond to small, intermediate and large mixing.

Table 5: Lower limits (95% CL) for the h^0 and A^0 bosons masses for various MSSM parameter scenarios. The limits are valid for any $\tan\beta$ larger than the value indicated and for any top quark mass smaller than the value indicated. If, in the case of small and intermediate mixing, the lower limit of $\tan\beta$ is decreased to 0.8, the limit of m_{h^0} remains unchanged and the limit of m_{A^0} vanishes for all values of m_t that have been considered. In the case of large mixing, this situation occurs already for $\tan\beta \geq 0.9$.

Squark mixing	$\tan\beta$	m_t (GeV)	$m_{h^0}^{lim}$	$m_{A^0}^{lim}$
Small mixing	1.0	195	44.8	27.5
	1.0	185	44.8	39.0
	1.0	175	44.8	44.8
	0.9	195	44.8	0.0
	0.9	185	44.8	9.3
	0.9	175	44.8	16.0
Intermediate mixing	1.0	195	44.3	39.0
	1.0	185	44.3	40.5
	1.0	175	44.3	41.0
	0.9	195	44.3	24.1
	0.9	185	44.3	24.1
	0.9	175	44.3	24.0
Large mixing	1.0	195	44.5	23.5
	1.0	185	44.5	23.8
	1.0	175	44.5	25.9

6 Summary

New results are presented from searches for neutral Higgs bosons in the SM and in the MSSM. The searches for the processes $Z^0 \to H^0 Z^*$ (SM) and $Z^0 \to h^0 Z^*$ (MSSM) use all data collected up to 1995 by the OPAL experiment in the vicinity of the Z^0 resonance, corresponding to an integrated luminosity of approximately 160 pb^{-1}.

The selection cuts in the missing energy and in the charged lepton channels have been optimized for good rejection of backgrounds and for high detection efficiencies for large Higgs bosons masses. In the charged lepton channel a detailed study of the residual backgrounds, mainly from four-fermion processes, has led to the conclusion that this channel still has the required sensitivity, and should not be discarded on the basis of excessive background. For that reason the limit is given for the missing energy channel and charged lepton channel combined, taking into account the observed $\mu^+\mu^- q\bar{q}$ event, with recoil mass 61.2 ± 1.0 GeV, as a Higgs boson candidate. This leads to a 95% CL lower limit of 59.6 GeV for the mass of the SM Higgs

boson. Had one used the missing energy channel alone, the result would be 60.6 GeV.

The same procedure is applied in deriving mass limits for the MSSM Higgs bosons h^0 and A^0. In contrast to earlier publications, the present limits are obtained in a more general theoretical framework of the MSSM where the Higgs boson masses and couplings (decay branching ratios) are obtained by solving the renormalization group equations at the two-loop level and where most relevant model parameters are varied over large ranges. A lower limit of 44.3 GeV (95% CL) is obtained for the mass of the lightest CP-even Higgs boson, h^0, almost independently of the MSSM model parameters. For $\tan\beta \geq 1$ and $m_t < 195$ GeV, the most conservative mass limit for the CP-odd Higgs boson, $m_{A^0} \geq 23.5$ GeV (95% CL), is obtained in the scenario with large squark mixing.

Acknowledgements:

We would like to acknowledge the help of Francesca Borzumati for clarifying some rather involved aspects of the MSSM parameter space.

We particularly wish to thank also the SL Division for the efficient operation of the LEP accelerator and for their continuing close cooperation with our experimental group.In addition to the support staff at our own institutions we are pleased to acknowledge the
Department of Energy, USA,
National Science Foundation, USA,
Particle Physics and Astronomy Research Council, UK,
Natural Sciences and Engineering Research Council, Canada,
Israel Ministry of Science,
Israel Science Foundation, administered by the Israel Academy of Science and Humanities,
Minerva Gesellschaft,
Japanese Ministry of Education, Science and Culture (the Monbusho) and a grant under the Monbusho International Science Research Program,
German Israeli Bi-national Science Foundation (GIF),
Direction des Sciences de la Matière du Commissariat à l'Energie Atomique, France,
Bundesministerium für Bildung, Wissenschaft, Forschung und Technologie, Germany,
National Research Council of Canada,
Hungarian Foundation for Scientific Research, OTKA T-016660,

References

[1] S. L. Glashow, J. Iliopoulos and L. Maiani, Phys. Rev. **D2** (1970) 1285;
S. Weinberg, Phys. Rev. Lett. **19** (1967) 1264;
A. Salam, *Elementary Particle Theory*, ed. N. Svartholm (Almquist and Wiksells, Stockholm, 1968), 367.

[2] P. W. Higgs, Phys. Lett. **12** (1964) 132;
F. Englert and R. Brout, Phys. Rev. Lett. **13** (1964) 321;
G. S. Guralnik, C. R. Hagen, and T. W. B. Kibble, Phys. Rev. Lett. **13** (1964) 585.

[3] J. Bjorken, *Proceedings of the 1976 SLAC Summer Institute on Particle Physics*, SLAC-198 (1977) 1.

[4] Y. Gol'fand and E. Likhtam, JETP Lett. **13** (1971)323;
D. Volkov and V. Akulov, Phys. Lett. **B46** (1973) 109;
J. Wess and B. Zumino, Nucl. Phys. **B70** (1974) 39;
H.E. Haber and Y. Nir, Nucl. Phys **B335** (1990) 363.

[5] H. P. Nilles, Phys. Rep. **110** (1984) 1;
H. E. Haber and G. L. Kane, Phys. Rep. **117** (1985) 75;
R. Barbieri *et al.*, Z. Physics at LEP1, CERN 89-08 (1989) Vol. 2, 121;
J.M. Frere, G.L. Kane, Nucl. Phys. **B223** (1983) 331;
J. Ellis *et al.*, Phys. Lett. **B123** (1983) 436;
J. Ellis *et al.*, Phys. Lett. **B127** (1983) 233.

[6] P. H. Chankowski, S. Pokorski and J. Rosiek, Phys. Lett. **B274** (1992) 191; Phys. Lett. **B281** (1992) 100; Phys. Lett. **B286** (1992) 307.

[7] E. Accomando *et al.*, *Higgs Physics* in *Physics at LEP2*, Editors: G. Altarelli, T. Sjöstrand and F. Zwirner, CERN 96-01 (1996).

[8] ALEPH Collaboration, D. Buskulic *et al.*, Phys. Lett. **B313** (1993) 299;
DELPHI Collaboration, P. Abreu *et al.*., Nucl. Phys. **B421** (1994) 3;
L3 Collaboration, O. Adriani *et al.*, Phys. Lett. **B303** (1993) 391.

[9] OPAL Collaboration, M. Z. Akrawy *et al.*, Phys. Lett. **B236** (1990) 224;
OPAL Collaboration, M. Z. Akrawy *et al.*, Phys. Lett. **B251** (1990) 211;
OPAL Collaboration, M. Z. Akrawy *et al.*, Zeit. f. Phys. **C49** (1991) 1;
OPAL Collaboration, P. D. Acton *et al.*, Phys. Lett. **B268** (1991) 122.

[10] OPAL Collaboration, R. Akers *et al.*, Phys. Lett. **B327** (1994) 397.

[11] ALEPH Collaboration, D. Buskulic *et al.*, Phys. Lett. **B313** (1993) 312;
DELPHI Collaboration, P. Abreu *et al.*., Z. Phys. **C67** (1995) 69;
L3 Collaboration, O. Adriani *et al.*., Z. Phys. **C57** (1993) 355.

[12] OPAL Collaboration, R. Akers *et al.*, Z. Phys. **C64** (1994) 1.

[13] M. Pohl, *Search for New Particles and New Interactions*, in Proceedings of the XXVIIth International Conference on High Energy Physics, Glasgow, Scotland, U.K., 20-27 July 1994, Eds. P. J. Bussey and I. G. Knowles, pp. 107-118.

[14] J.-F. Grivaz, *New Particle Searches*, in Proceedings of the International Europhysics Conference on High Energy Physics, Brussels (Belgium), July 27 - August 2, 1995.

[15] ALEPH Collaboration, D. Buskulic *et al.*, CERN-PPE/96-079 (17 June 1996).

[16] OPAL Collaboration, G. Alexander *et al.*, Phys. Lett. **B377** (1996) 273.

[17] Y. Okada, M. Yamaguchi and T. Yanagida, Prog. Theor. Phys. Lett. **85** (1991) 1; Phys. Lett. **B262** (1991) 54;
A. Yamada, Phys. Lett. **B263** (1991) 233;
J. Ellis, G. Ridolfi, F. Zwirner, Phys. Lett. **B258** (1991) 167; Phys. Lett. **B262** (1991) 477, and references therein;
H. E. Haber and R. Hempfling, Phys. Rev. Lett. **66** (1991) 1815;
A. Brignole and F. Zwirner, Phys. Lett. **B299** (1993) 72;
A. Brignole, J. Ellis, G. Ridolfi and F. Zwirner, Phys. Lett. **B271** (1991) 123;
H. E. Haber, R. Hempfling and Y. Nir, Phys. Rev. **D46** (1992) 3015;
R. Barbieri and M. Frigeni, Phys. Lett. **B258** (1991) 395;
A. Brignole *et al.*, Phys. Lett. **B271** (1991) 123.

[18] M. Carena, K. Sasaki and C.E.M. Wagner, Nucl. Phys. **B381** (1992) 66;
P. H. Chankowski, S. Pokorski and J. Rosiek, Phys. Lett. **B281** (1992) 100.

[19] CDF Collaboration, F. Abe *et al.*, Phys.Rev.Lett.**74** (1995) 2626;
D0 Collaboration, S. Abachi *et al.*, Phys.Rev.Lett.**74** (1995) 2632.

[20] OPAL Collaboration, K. Ahmet *et al.*, Nucl. Inst. and Meth. **A305** (1991) 275.

[21] P. P. Allport *et al.*, Nucl. Inst. and Meth. **A324** (1993) 34;
P. P. Allport *et al.*, Nucl. Inst. and Meth. **A346** (1994) 476.

[22] B.E. Anderson *et al.*, IEEE Transactions on Nuclear Science **41** (1994) 845.

[23] J. Allison *et al.*, Nucl. Inst. and Meth. **A317** (1992) 47.

[24] PYTHIA 5.7 and JETSET 7.4, T. Sjöstrand, Comp. Phys. Comm. **82** (1994) 74;
T. Sjöstrand, LU TP 95-20 and CERN-TH.7112/93 (revised August 1995).

[25] OPAL Collaboration, G. Alexander *et al.*, Z. Phys. **C69** (1996) 543.

[26] J. Hilgart, R. Kleiss and F. Le Diberder, Comp. Phys. Comm. **75** (1993) 191.

[27] OPAL Collaboration, G. Alexander *et al.*, Phys. Lett. **B376** (1996) 315.

[28] OPAL Collaboration, M. Z. Akrawy *et al.*, Phys. Lett. **B253** (1991) 511.

[29] OPAL Collaboration, R. Akers *et al.*, Z. Phys. **C65** (1995) 17.

[30] E. Accomando *et al.*, *Event generators for discovery physics* in *Physics at LEP2*, Editors: G. Altarelli, T. Sjöstrand and F. Zwirner, CERN 96-01 (1996).

[31] M. Carena, M. Quiros and C. E. M. Wagner, Nucl. Phys. **B461** (1996) 407.

[32] OPAL Collaboration, G. Alexander *et al.*, Phys. Lett. **B377** (1996) 181.

[33] D. Schaile, Fortschritte der Physik, **42** (1994) 429.

[34] OPAL Collaboration, M. Z. Akrawy *et al.*, Phys. Lett. **B240** (1990) 261; Phys. Lett. **B252** (1990) 290.

[35] OPAL Collaboration, R. Akers *et al.*, Phys. Lett. **B337** (1994) 207.

[36] J. Rosiek and A. Sopczak, Phys. Lett. **B341** (1995) 419.

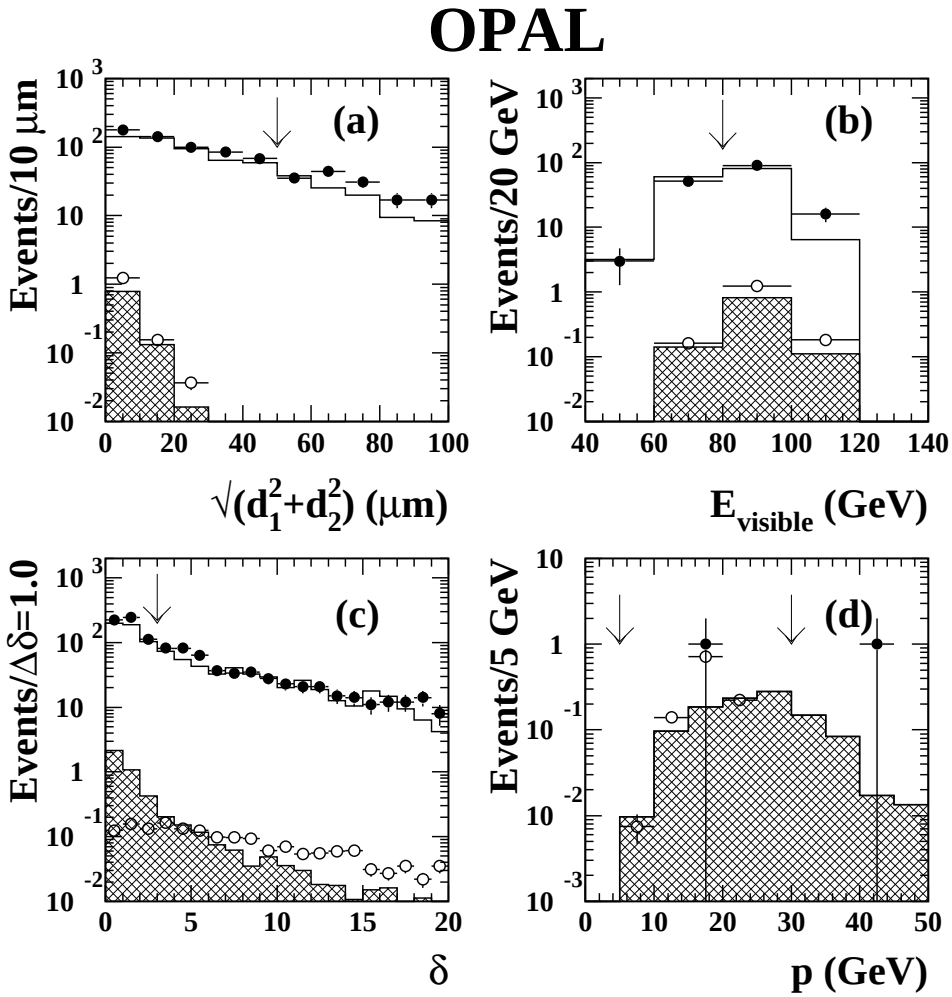

Figure 1: Distributions for the new cut variables for the e^+e^- and $\mu^+\mu^-$ channels together. (a) The distribution of $\sqrt{d_1^2 + d_2^2}$ after all cuts except the one applied to that quantity and the lepton isolation cuts; (b) the visible energy distribution after all cuts except the one applied to that quantity and with the lepton isolation cuts loosened; (c) the distribution of $\delta \equiv \ell/\sigma_\ell$, after all cuts except the one applied to that quantity and the lepton isolation cuts; (d) the higher of the two lepton momenta after all cuts except the one applied to the lepton momenta. In all plots the data are shown by solid points. The arrows show the position of the cuts. The open histogram is the sum for the multihadronic and four-fermion backgrounds. The shaded histograms show the four fermion background alone. The signal for a Higgs boson with 60 GeV mass is shown by the open points.

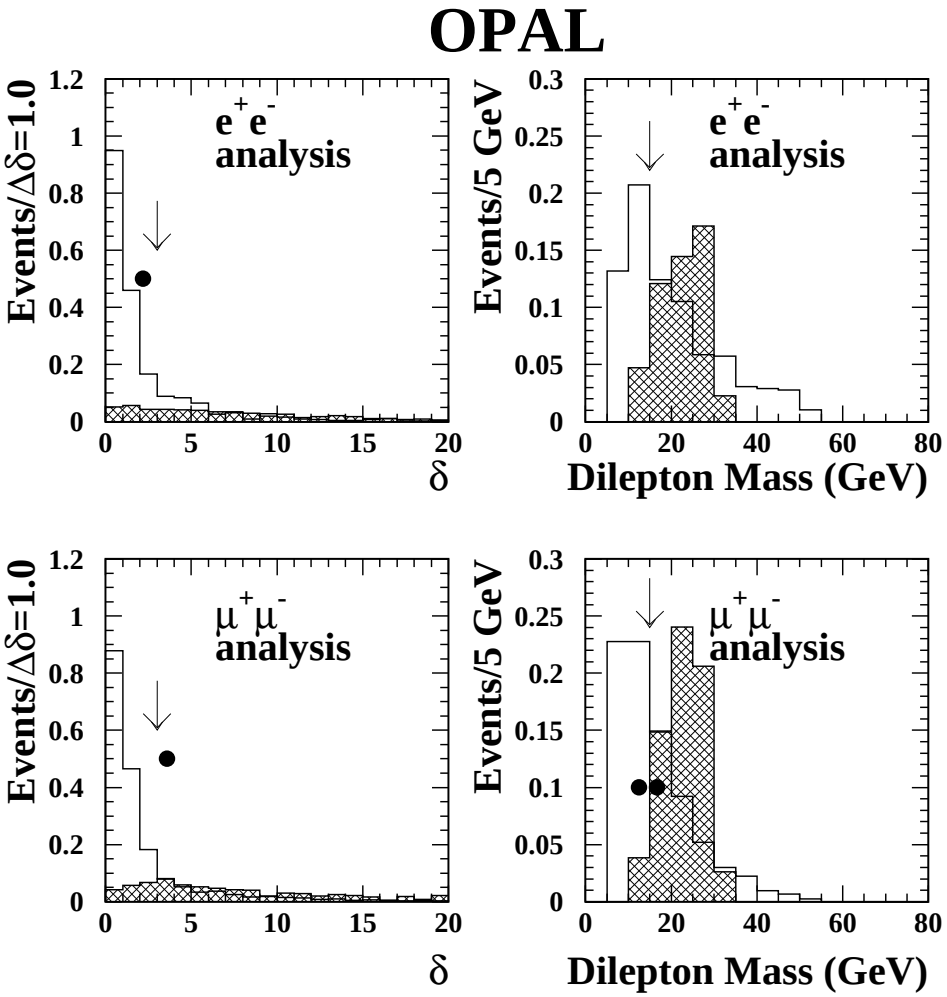

Figure 2: Distribution of $\delta \equiv \ell/\sigma_\ell$ and of the dilepton mass spectra after all cuts except those applied to the quantities displayed. The white histograms show the four-fermion background and the shaded histograms the signal for a Higgs boson with 60 GeV mass. The solid dots represent the data. Events to the right of the arrows are accepted.

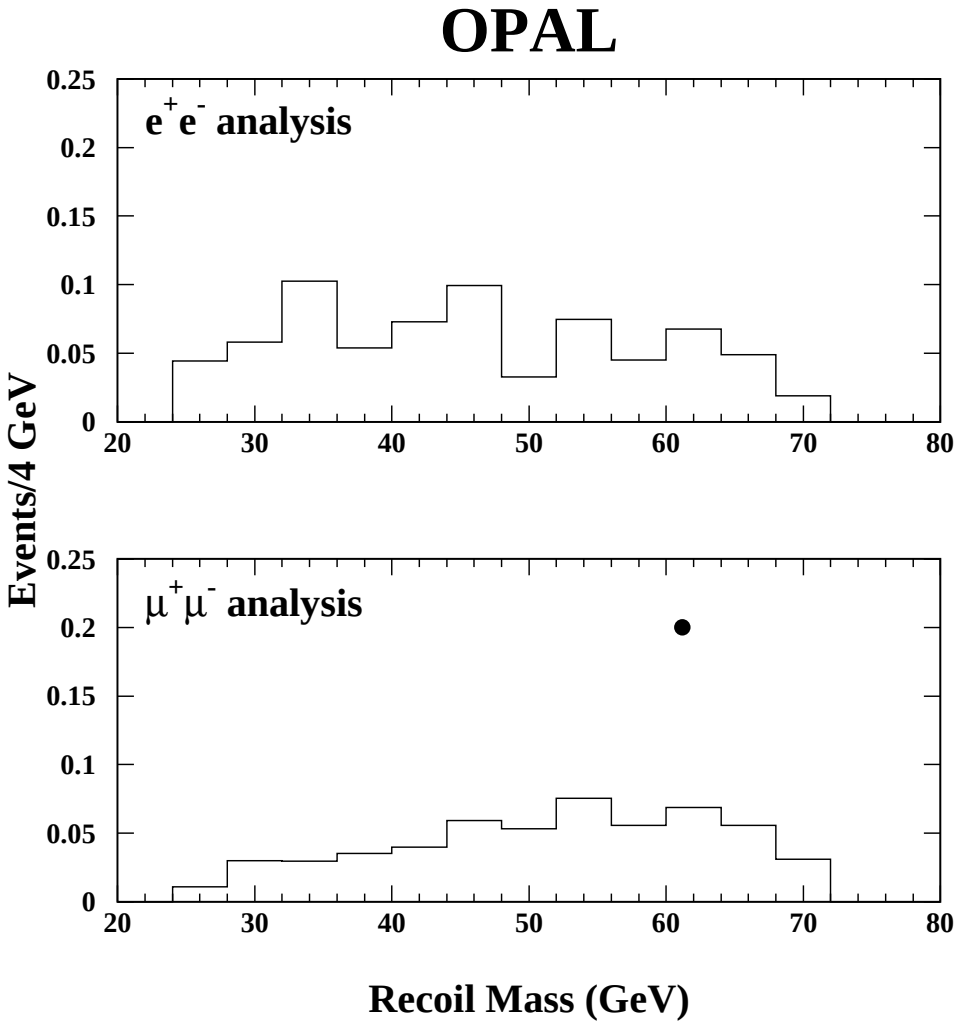

Figure 3: Recoil mass distributions for the background after all cuts. Since hadronic Z^0 decays have been removed completely, only the background from four-fermion processes contributes to the distributions. The dot shows the event in the $\mu^+\mu^-$ channel, with 61.2 ± 1.0 GeV mass, that passed the cuts.

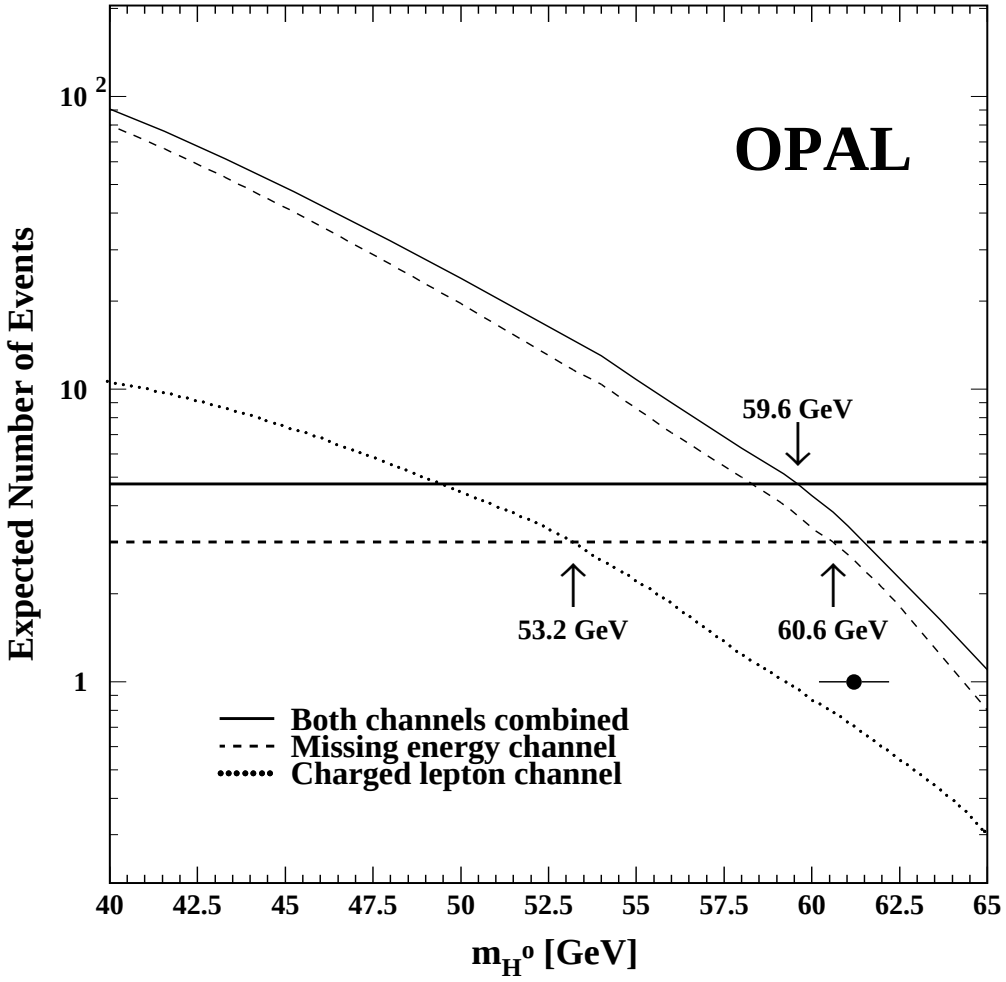

Figure 4: Derivation of the mass limit for the SM Higgs boson. The curves represent the predicted number of observable Higgs boson events, decreased by their systematic errors, in the charged lepton channel (dotted line), in the missing energy channel (dashed line) and in both channels combined (full line). The horizontal lines indicate the 95% CL upper limits for a possible signal in the case of zero observed event (dashed line) and in the case of one observed event (full line). The arrows indicate mass limits from the missing energy channel and charged lepton channel separately and from the two channels combined. The event observed in the $\mu^+\mu^-$ channel, with 61.2 ± 1.0 GeV mass, is indicated by the solid dot with error bars.

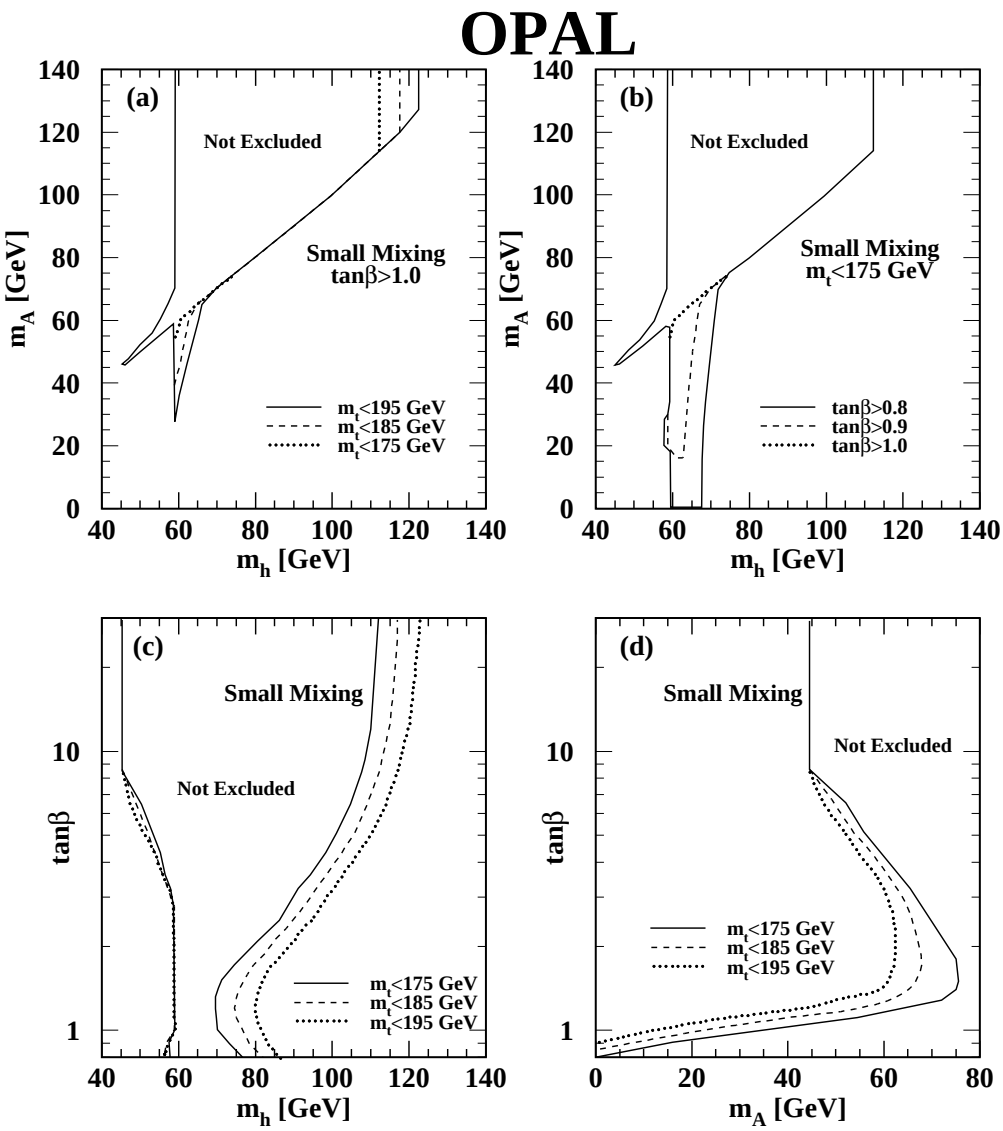

Figure 5: Exclusion contours valid at the 95% CL obtained for MSSM parameter combinations which correspond to $A = 0$ and $\mu = -50$ GeV (small mixing scenario). (a) Projection on the (m_{h^0},m_{A^0}) plane, for $\tan\beta > 1$ and for three upper limits of the top quark mass. (b) Projection on the (m_{h^0}, m_{A^0}) plane, for the upper limit of the top quark mass fixed at 175 GeV and for three lower limits of $\tan\beta$. (c) Projection on the (m_{h^0},$\tan\beta$) plane, for three upper limits of the top quark mass. (d) Projection on the (m_{A^0},$\tan\beta$) plane, for three upper limits of the top quark mass.

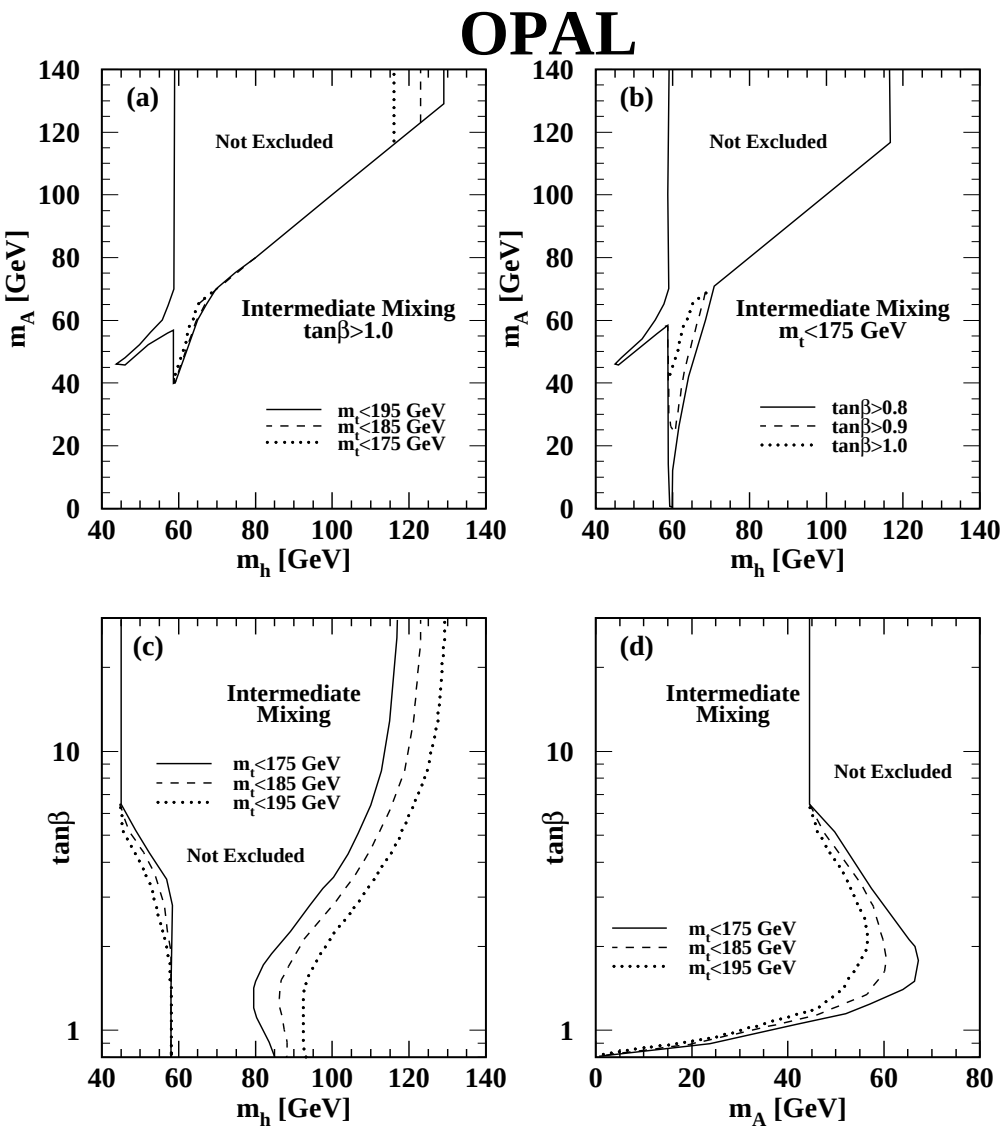

Figure 6: Exclusion contours valid at the 95% CL obtained for MSSM parameter combinations which correspond to $A = M_S$ and $\mu = -M_S$ (intermediate mixing scenario). (a) Projection on the (m_{h^0},m_{A^0}) plane, for $\tan\beta > 1$ and for three upper limits of the top quark mass. (b) Projection on the (m_{h^0}, m_{A^0}) plane, for the upper limit of the top quark mass fixed at 175 GeV and for three lower limits of $\tan\beta$. (c) Projection on the (m_{h^0},$\tan\beta$) plane, for three upper limits of the top quark mass. (d) Projection on the (m_{A^0},$\tan\beta$) plane, for three upper limits of the top quark mass.

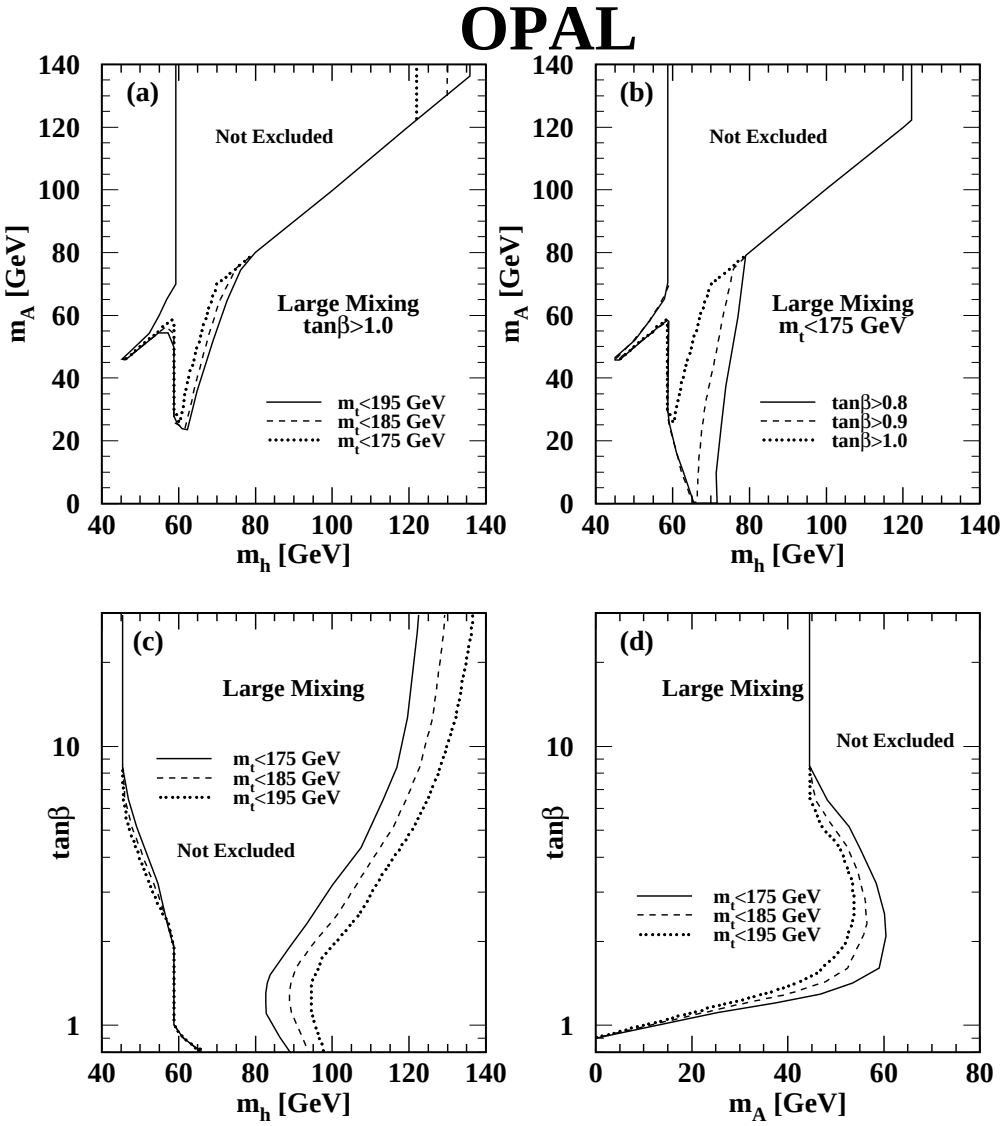

Figure 7: Exclusion contours valid at the 95% CL obtained for MSSM parameter combinations which correspond to $A = M_S\ \sqrt{6}$ and $\mu = -50$ GeV (large mixing scenario). (a) Projection on the (m_{h^0},m_{A^0}) plane, for $\tan\beta > 1$ and for three upper limits of the top quark mass. (b) Projection on the (m_{h^0}, m_{A^0}) plane, for the upper limit of the top quark mass fixed at 175 GeV and for three lower limits of $\tan\beta$. (c) Projection on the (m_{h^0},$\tan\beta$) plane, for three upper limits of the top quark mass. (d) Projection on the (m_{A^0},$\tan\beta$) plane, for three upper limits of the top quark mass.